Thermodynamic Study of Phosphoglycerate Kinase from *Thermotoga maritima* and Its Isolated Domains: Reversible Thermal Unfolding Monitored by Differential Scanning Calorimetry and Circular Dichroism Spectroscopy†

Katrin Zaiss and Rainer Jaenicke*

Institut für Biophysik und Physikalische Biochemie, Universität Regensburg, D-93040 Regensburg, Germany

Received October 14, 1998; Revised Manuscript Received January 21, 1999

ABSTRACT: The folding of phosphoglycerate kinase (PGK) from the hyperthermophilic bacterium *Thermotoga maritima* and its isolated N- and C-terminal domains (N1/2 and C1/2) was characterized by differential scanning calorimetry (DSC) and circular dichroism (CD) spectroscopy. At pH 3.0−4.0, reversible thermal denaturation of TmPGK occurred below 90 °C. The corresponding peaks in the partial molar heat capacity function were fitted by a four-state model, describing three well-defined unfolding transitions. Using CD spectroscopy, these are ascribed to the disruption of the domain interactions and subsequent sequential unfolding of the two domains. The isolated N-terminal domain unfolds reversibly between pH 3.0 and pH 4.0 to >90% and at pH 7.0 to about 70%. In contrast, the isolated engineered C-terminal domain only shows reversible thermal denaturation between pH 3.0 and pH 3.5. Neither N1/2 nor C1/2 obeys the simple two-state mechanism of unfolding. Instead, both unfold via a partially structured intermediate. In the case of N1/2, the intermediate exhibits native secondary structure and perturbed tertiary structure, whereas for C1/2 the intermediate could not be defined with certainty.

Studies on the reversible unfolding of proteins have been performed for a long time to answer the question, what is the molecular basis of protein stability (*1*)? In this context, reversible thermal denaturation has been of great importance, since the free energy of stabilization can be determined directly using statistical thermodynamics, without any assumptions regarding the influence of other denaturants. The best approach to obtain thermodynamic information, even on complex unfolding transitions, is DSC.[1] It is the only method that allows the direct determination of the enthalpy associated with the reversible denaturation of proteins (*2*, *3*). All temperature-induced changes in macroscopic systems proceed with a well-defined change of enthalpy, since enthalpy and temperature are coupled extensive and intensive variables. The functional relation between these variables includes all the thermodynamic information about the macroscopic states which are populated in the process of denaturation. The temperature dependence of the enthalpy function can be determined experimentally by calorimetric measurements of the heat capacity, since the heat capacity at constant pressure is the first temperature derivative of the enthalpy function, described by the Kirchhoff equation (*3*−*5*).

DSC allows (i) to decide whether a thermal denaturation can be described by a two-state model, (ii) to calculate the thermodynamic functions of the denaturation reaction, and (iii) to analyze single steps of a complex denaturation reaction. In order to correlate these thermodynamic data with certain specific regions or structural elements of a protein, other methods such as spectroscopy or chemical modification have to be applied. In this connection, CD spectroscopy has been of importance, since the appropriate choice of the wavelength in the near- or far-UV allows structural changes at the level of the tertiary or secondary structure to be determined.

Compared to the numerous studies on small monomeric proteins investigated by DSC in the past, PGK is a highly complex system. The monomeric protein from *Thermotoga maritima* has a molecular mass of 43 kDa and consists of two well-separated domains undergoing a dramatic hinge motion in the catalytic mechanism (*6*−*9*). As a consequence of the mobility of the domains, intrinsic stability must be established within each of the domains and cannot be expected from interdomain contacts.

In contrast to the enzyme from yeast, which is inaccessible to reversible denaturation unless GdmCl is added (*10*−*12*), TmPGK shows reversible thermal denaturation at pH 3−4. In the present study, intact TmPGK and its engineered isolated N- and C-terminal domains were characterized by thermal and spectral analysis, addressing the following questions: Can the folding of the isolated domains be described by a two-state model? Does the self-organization of intact TmPGK involve separate folding and subsequent

† This work was supported by the Deutsche Forschungsgemeinschaft (Grant Ja 78/34-1) and by the Fonds der Chemischen Industrie.

* Author to whom correspondence should be addressed.

[1] Abbreviations: C1/2, C-terminal domain of TmPGK (Met + Ile175−Lys399); CD, circular dichroism; $\Delta C_{p,i}$, change in the partial molar heat capacity connected with the *i*th transition; ΔG_i, free energy of the *i*th transition; ΔH_i, enthalpy change of the *i*th transition; DSC, differential scanning calorimetry; *E. coli*, *Escherichia coli*; GdmCl, guanidinium chloride; IEP, isoelectric point; N1/2, N-terminal domain of TmPGK (Met1−Ile175); PGK, phosphoglycerate kinase (EC 2.7.2.3); $T_{m,i}$, transition temperature of the *i*th transition; Tm, *Thermotoga maritima.*

10.1021/bi982447e CCC: $18.00
Published on Web 03/19/1999

pairing of its domains? What can we learn about the stability of the isolated domains in comparison with the stability of the intact two-domain protein?

EXPERIMENTAL PROCEDURES

Materials. All chemicals were of analytical grade and bidistilled water was used throughout.

Protein Purification. Recombinant TmPGK was purified to homogeneity as described by Grättinger et al. (*13*). The recombinant isolated domains of TmPGK, N1/2 (Met1−Ile175) and C1/2 (Met + Ile175−Lys399), were cloned in *Escherichia coli* and purified to homogeneity as described (*14*).

Protein Concentration. Protein concentrations were determined by measuring the absorption at 280 nm in a Cary 1/3 Varian UV absorption spectrophotometer at 20 °C. The following absorption coefficients were used: $A_{0.1\%,1cm,280nm} = 0.51 \pm 0.3$ for intact TmPGK (*13*) and $A_{0.1\%,1cm,280nm} = 0.38 \pm 0.1$ and 0.63 ± 0.01 for N1/2 and C1/2, respectively (*14*).

Protein Stability. (A) pH. For the pH profiles, aliquots of the protein solutions were incubated for at least 24 h at 20 °C in the following buffers: 20 mM glycine/HCl, pH 2.5, 3.0, 3.6; 20 mM sodium acetate, pH 3.6, 4.1, 4.6, 5.2; 20 mM sodium cacodylate/HCl, pH 5.2, 5.8, 6.4, 7.0; 20 mM Tris/HCl, pH 7.0, 7.5, 8.0, 8.6; 20 mM glycine/NaOH, pH 8.6, 9.2, 9.8, 10.5; 20 mM Na_2HPO_4/NaOH, pH 11.0, 11.5. Protein concentrations were ca. 20 μg/mL. pH profiles were recorded by fluorescence emission ($\lambda_{exc} = 280$ nm) at 3.15 nm for N1/2 and at 365 nm for C1/2 using a Spex Fluoromax (Instruments S.A.) or a Perkin-Elmer MPF-3l spectrophotometer equipped with a thermostated cell holder at 20 °C.

(B) Temperature. Temperature-induced equilibrium unfolding transitions were investigated by making use of DSC and CD spectroscopy. For these measurements the following buffers were used: 20 mM glycine/HCl at pH 3.0−3.5, 20 mM sodium acetate (NaOAc/HAc) at pH 3.5−4.0, and 20 mM sodium phosphate (Na_2HPO_4/NaH_2PO_4) at pH 7.0.

(1) DSC measurements made use of a Nano-DSC CSC 5100 calorimeter (*15*) at a constant heating rate of 1 K/min, if not stated otherwise. All samples were dialyzed against a 1000-fold volume of buffer for at least 16 h. An aliquot of the dialysis buffer was filtrated and degassed by evacuation. Protein solutions were centrifuged in an Eppendorf centrifuge for at least 10 min at 15800*g*, 4 °C, and carefully degassed before the protein concentration was determined. In order to improve the baseline stability, buffer baselines were repeated several times before the protein was scanned. Baselines and samples were measured under identical conditions. To improve the reversibility, the first heating was stopped right after the transition; the degree of reversibility was assessed by reheating the sample.

The data were analyzed using the deconvolution software CpCalc Analysis (version 2.1) of the CSC 5100 (*15*). After subtraction of the instrumental baseline and transformation of the raw data into partial molar heat capacities, curves were fitted to the equation:

$$C_p = C_{p,0} + \frac{\partial}{\partial T}\left(\sum_{i=1}^{N} P_i \Delta H_i\right)$$

in which C_p is the partial molar heat capacity, $C_{p,0}$ is the partial molar heat capacity of the native state, T is the temperature, P_i is the population of the ith state, ΔH_i is the enthalpy difference between the ith state and the native state, and N is the number of transitions.

Evaluation of the data on the basis of equilibrium thermodynamics is only allowed if the system is in equilibrium throughout the whole transition. This was determined for each protein by testing the independence of the scan rate (0.5, 1.0, and 2.0 K/min) under defined conditions. For all three proteins, no influence of the scan rate on the partial molar heat capacity was detectable (data not shown).

(2) CD "melting curves" were monitored using an AVIV 62DS spectropolarimeter with a thermostated cell holder. To accomplish an effective scan rate of about 1 K/min, every 1 °C the signal was integrated for 10 s at a constant wavelength. The bandwidth was 1 nm; a temperature deviation of 0.1 °C was tolerated.

The concentration of the protein samples was adjusted to an absorbance of 0.8 at 280 nm using a 1 cm quartz cuvette. In the near-UV, samples at the initial concentration were measured in a 1 cm quartz cell with Teflon stopper. In the far-UV, aliquots of the protein were diluted 1:10 with the reference buffer; a 0.1 cm quartz cell with Teflon stopper was used for the measurements. To further prevent evaporation, samples were overlayed with mineral oil. All measurements were corrected for the contributions of the solvent.

(C) GdmCl. GdmCl-induced equilibrium transitions were determined by incubating the proteins at varying denaturant concentrations for at least 24 h at 20 °C. For refolding experiments, the proteins were denatured for at least 3 h at room temperature in 5.1 M GdmCl for N1/2 and 4.3 M for C1/2. Measurements were performed in 20 mM sodium phosphate, pH 7.0, and protein concentrations were 25 μg/mL N1/2 and 35 μg/mLC1/2. The transitions were monitored by fluorescence emission spectroscopy ($\lambda_{exc} = 280$ nm) recorded at 315 nm for N1/2 and 365 nm for C1/2 using a Spex Fluoromax (Instruments S.A.) or Perkin-Elmer MPF-3l spectrophotometer equipped with a thermostated cell holder at 20 °C.

RESULTS

Molecular properties of TmPGK and its isolated N- and C-terminal domains may be summarized as follows: All three proteins are monomeric at neutral and acidic pH. Absorption, fluorescence emission, and circular dichroism spectroscopy indicate that the recombinant isolated domains are in their native state. Substrate binding experiments confirm this finding. No reconstitution of N1/2 and C1/2 to form the "nicked" two-domain protein was observed (data not shown; cf. ref 14).

TmPGK and its isolated domains undergo reversible thermal denaturation at pH 3−4. Under these conditions all three proteins still exhibit native spectral characteristics. However, they are sufficiently destabilized so that complete thermal unfolding in DSC experiments is accomplished within the temperature regime below 100 °C. Representative examples of pH profiles and selected fluorescence spectra of the isolated domains are shown in Figure 1. N1/2 is native from pH 3.0 to pH 11.5, as suggested by the form of the spectra and the wavelength of maximum emission; at pH

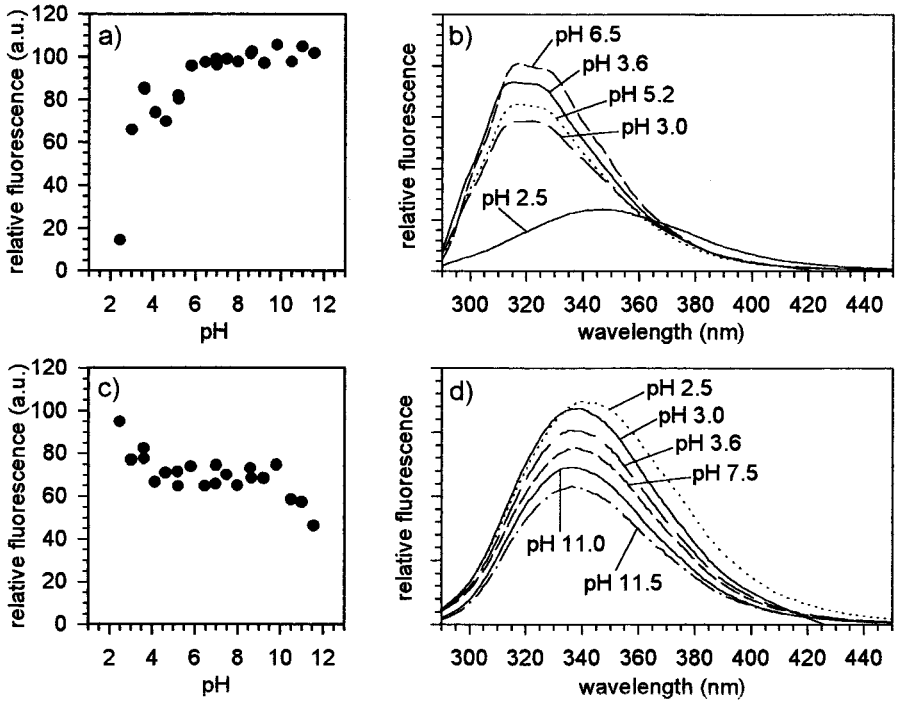

FIGURE 1: N1/2: pH−stability profiles monitored by fluorescence emission at 315 nm (a) and selected fluorescence emission spectra (b). C1/2: pH−stability profiles monitored by fluorescence emission at 365 nm (c) and selected fluorescence emission spectra (d) ($\lambda_{exc} = 280$ nm). Buffers: 20 mM glycine/HCl, pH 2.5, 3.0, 3.6; 20 mM sodium acetate, pH 3.6, 4.1, 4.6, 5.2; 20 mM sodium cacodylate/HCl, pH 5.2, 5.8, 6.4, 7.0; 20 mM Tris/HCl, pH 7.0, 7.5, 8.0, 8.6; 20 mM glycine/NaOH, pH 8.6, 9.2, 9.8, 10.5; 20 mM Na_2HPO_4/NaOH, pH 11.0, 11.5.

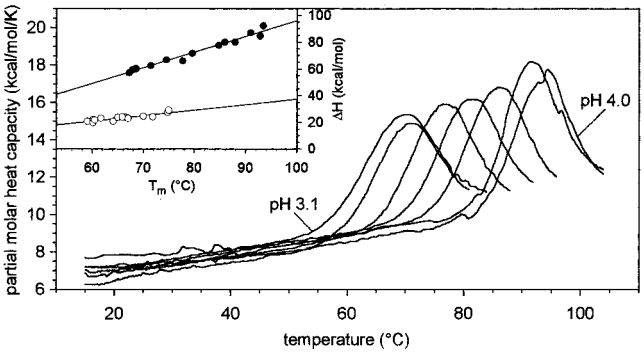

FIGURE 2: DSC scans of N1/2 at pH 3.1, 3.2, 3.3, 3.4, 3.5, 3.7, and 4.0 (from left to right). Insert: ΔH vs T_m plot for the first (○) and second (●) transition of the DSC scans (ΔH_i and $T_{m,i}$ values result from the deconvolution of the DSC scans; cf. Table 1). The gradients of the linear regression yield $\Delta C_{p,1} = 0.4 \pm 0.2$ kcal mol^{-1} K^{-1} ($r^2 = 0.79$) and $\Delta C_{p,2} = 1.2 \pm 0.2$ mol^{-1} K^{-1} ($r^2 = 0.97$), respectively.

Table 1: Thermodynamic Parameters for N1/2 Calculated by Deconvolution of DSC Scans at Various pH Values[a]

pH	concn (mg/mL)	$T_{m,1}$ (°C)	ΔH_1 (kcal/mol)	$\Delta C_{p,1}$ (kcal mol^{-1} K^{-1})	$T_{m,2}$ (°C)	ΔH_2 (kcal/mol)	$\Delta C_{p,2}$ (kcal mol^{-1} K^{-1})	reversibility (%)
3.1	2.19	59.1	20.7	0.6	67.9	59.2	1.4	96
3.2	1.36	60.2	22.0	0.4	68.5	60.4	1.7	100
3.2[b]	1.38	60.2	19.7	0.4	67.2	57.1	2.4	nd
3.2[c]	1.31	60.5	21.6	0.5	68.6	60.2	1.7	nd
3.2	1.47	61.7	22.9	0.3	71.5	62.3	0.4	100
3.3	2.71	65.9	24.0	0.8	77.7	65.9	0.7	90
3.3	1.40	64.1	20.6	0.4	74.5	66.6	1.8	98
3.4	1.39	65.0	23.7	0.3	79.6	71.4	1.8	95
3.5	2.82	67.0	22.8	0.4	85.9	80.0	2.4	96
3.5	1.32	66.6	23.6	0.5	84.7	77.5	1.7	93
3.7	2.22	69.7	21.9	0.6	88.0	80.6	2.2	92
3.7	1.94	70.0	24.5	0.5	91.0	87.1	1.9	94
4.0	1.28	75.0	28.9	0.4	93.4	92.2	2.0	94
4.0	1.32	74.8	27.2	0.5	92.8	84.6	1.8	nd

[a] The error limits for T_m and ΔH are about 1% and 5%, respectively. [b] Scan rate 0.5 K/min. [c] Scan rate 2.0 K/min.

2.5, N1/2 is denatured. The loss of fluorescence intensity below pH 4.0 might be due to protonation of Glu123, which is the only nonhydrophobic contact of the single tryptophan residue in N1/2. C1/2 is also native from pH 3.0 to pH 11.5. Beyond pH 9.8, the fluorescence intensity is partly quenched compared to the emission at neutral pH, probably caused by the titration of the solvent-exposed Trp291. Below pH 4, the intensity is increased without a significant red shift of the maximum wavelength. In this case, there is no clear correlation of the spectral change to specific titratable groups.

N1/2 Domain. DSC scans of N1/2 at pH 3.1−4.0 are shown in Figure 2. Only one broad peak for the change in the partial molar heat capacity was observed. The transition maximum strongly depends on the pH, varying from about 68 °C at pH 3.1 to 93 °C at pH 4.0. Deconvolution of the single thermal transitions showed that the folding of the N-terminal domain does not obey the two-state model. The profiles can only be fitted by a three-state model, yielding a first transition (marked by the subscript 1) with a rather small change in enthalpy and heat capacity and a second more distinct transition (subscript 2). The deconvolution results are summarized in Table 1. To improve the reversibility, the first heating scan was stopped right after the transitions. As reported previously, a missing posttransitional baseline or even truncation of the peak has no influence on the reliability of the fitted ΔH and T_m values (*16*, *17*). In the present case, only the deconvoluted ΔC_p values ($\Delta C_{p,1}$ and $\Delta C_{p,2}$) are unreliable, probably due to the missing posttransitional baseline. Therefore, the determination of the changes in the partial molar heat capacity was controlled by plotting ΔH vs T_m according to the Kirchhoff equation. The slopes in the insert of Figure 2 allow $\Delta C_{p,1} = 0.4 \pm 0.2$ kcal mol^{-1}

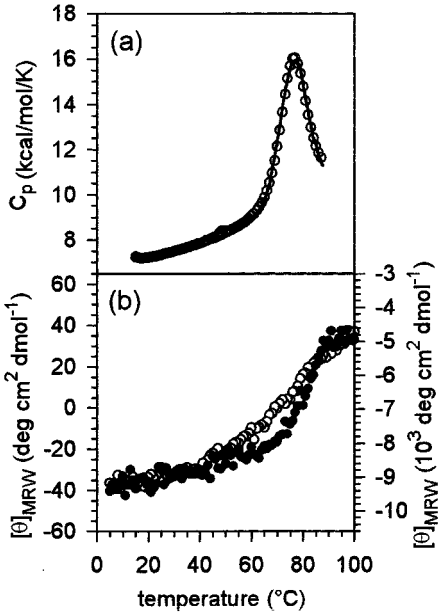

FIGURE 3: Temperature-induced transitions of N1/2 in 20 mM glycine/HCl, pH 3.3: (a) monitored by DSC (—) and fitted with a three-state model (○); (b) monitored by far- and near-UV CD [far-UV at 222 nm (●, right axis); near-UV at 275 nm (○, left axis)].

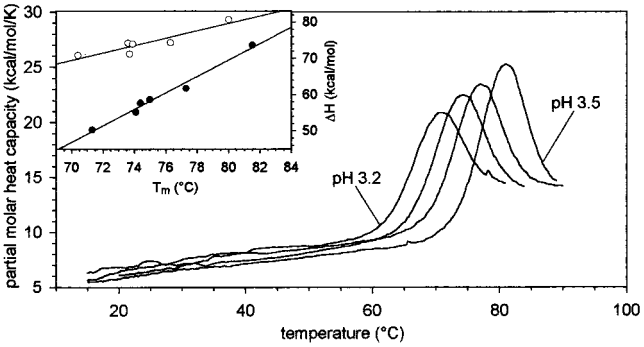

FIGURE 4: DSC scans of C1/2 at pH 3.2, 3.3, 3.4, and 3.5 (from left to right). Insert: ΔH vs T_m plot for the first (○) and second (●) transition of the DSC scans (ΔH_i and $T_{m,i}$ values result from the deconvolution of the DSC scans; cf. Table 2). The gradients of the linear regression yield $\Delta C_{p,1} = 1.0 \pm 0.2$ kcal mol^{-1} K^{-1} ($r^2 = 0.90$) and $\Delta C_{p,2} = 2.3 \pm 0.2$ kcal mol^{-1} K^{-1} ($r^2 = 0.98$), respectively.

K^{-1} and $\Delta C_{p,2} = 1.2 \pm 0.2$ kcal mol^{-1} K^{-1} to be calculated. To interpret the two transitions in structural terms, melting curves were monitored by near- and far-UV CD. As illustrated in Figure 3, the two melting curves of N1/2 are not superimposable. This suggests a sequential two-step unfolding of the tertiary and secondary structure, with perturbation of the tertiary structure as the first step and unfolding of the secondary structure as the second step.

C1/2 Domain. For C1/2, the pH range of reversible thermal denaturation is much narrower compared to the pH range for intact TmPGK or N1/2. Already at pH 3.6, the reversibility drops to less than 30%. Therefore, DSC measurements were restricted to the range between pH 3.2 and pH 3.5, where the yield of renaturation exceeds 90% (Figure 4). As in the case of N1/2, the peaks are again too broad to be fitted by a single transition; instead, two transitions with close transition temperatures are required to fit the DSC scans (Table 2). Again, plotting ΔH vs T_m yields two straight lines with slopes corresponding to $\Delta C_{p,1} = 1.0 \pm 0.2$ kcal mol^{-1}

Table 2: Thermodynamic Parameters for C1/2 Calculated by Deconvolution of DSC Scans at Various pH Values[a]

pH	concn (mg/mL)	$T_{m,1}$ (°C)	ΔH_1 (kcal/mol)	$\Delta C_{p,1}$ (kcal mol^{-1} K^{-1})	$T_{m,2}$ (°C)	ΔH_2 (kcal/mol)	$\Delta C_{p,2}$ (kcal mol^{-1} K^{-1})	reversibility (%)
3.2	1.34	70.4	70.8	1.0	71.3	50.3	1.0	95
3.3	1.25	73.6	74.2	1.0	74.4	57.7	1.0	93
3.3[b]	1.27	73.9	73.9	1.0	75.0	58.7	1.1	nd
3.3[c]	1.26	73.7	71.2	1.0	74.1	55.2	2.6	nd
3.4	1.29	76.3	74.3	1.0	77.3	61.7	1.0	90
3.5	1.23	80.0	80.7	1.0	81.5	73.7	0.8	95

[a] The error limits for T_m and ΔH are about 1% and 5%, respectively. [b] Scan rate 0.5 K/min. [c] Scan rate 2.0 K/min.

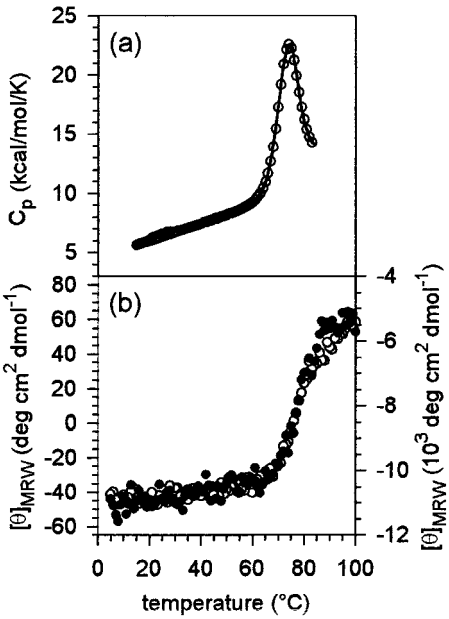

FIGURE 5: Temperature-induced transitions of C1/2 in 20 mM glycine/HCl, pH 3.3: (a) monitored by DSC (—) and fitted with a three-state model (○); (b) monitored by far- and near-UV CD [far-UV at 222 nm (●, right axis); near-UV at 269 nm (○, left axis)].

K^{-1} and $\Delta C_{p,2} = 2.3 \pm 0.2$ kcal mol^{-1} K^{-1} for the first and second transition (insert, Figure 4). No unequivocal structural interpretation can be deduced from the CD spectra. A representative example, recorded at pH 3.3, is shown in Figure 5, together with the corresponding DSC scan. In contrast to N1/2, the near- and far-UV CD transitions coincide. The two transition midpoints are too close to decide whether a hierarchical unfolding of the tertiary and secondary structure takes place or a sequential unfolding of subdomains with a simultaneous loss of the native tertiary and secondary structure.

Intact TmPGK. In proceeding from the isolated domains to intact TmPGK, a complex unfolding mechanism is expected. Figure 6 shows DSC scans for the enzyme at pH 3.0−4.0. Again, only a single peak is observed. Both the transition temperature and the cooperativity depend strongly on the pH; as one would predict, with increasing net charge the peaks become broader and are shifted to lower temperatures. Excluding the scans at pH ≤3.2, a four-state model is the only way to fit the ΔC_p data according to the Kirchhoff equation. This confirms the temperature-induced alterations of the dichroic absorption at 285 and 222 nm (Figure 7). The results of the deconvolution of the DSC scans are summarized in Table 3. The unfolding may be tentatively

Table 3: Thermodynamic Parameters for Intact TmPGK Calculated by Deconvolution of DSC Scans at Various pH Values[a]

pH	concn (mg/mL)	$T_{m,1}$ (°C)	ΔH_1 (kcal/mol)	$\Delta C_{p,1}$ (kcal mol^{-1} K^{-1})	$T_{m,2}$ (°C)	ΔH_2 (kcal/mol)	$\Delta C_{p,2}$ (kcal mol^{-1} K^{-1})	$T_{m,3}$ (°C)	ΔH_3 (kcal/mol)	$\Delta C_{p,3}$ (kcal mol^{-1} K^{-1})	reversibility (%)
3.1	1.18				60.5	59.3	2.1	66.3	69.9	2.1	96
3.2	0.93				63.4	63.3	1.8	69.7	81.5	1.7	94
3.3	1.33	55.9	24.5	1.5	69.0	70.7	1.7	72.4	83.9	2.7	86
3.4	0.69	57.0	35.7	2.2	71.0	71.0	1.7	75.1	93.2	2.7	96
3.4	0.98	64.8	51.7	2.1	74.6	75.7	1.7	77.7	94.0	2.1	98
3.5	1.89	65.9	43.8	1.9	75.6	77.5	1.5	77.8	89.3	2.3	90
3.5	1.31	68.8	50.4	1.5	75.2	78.8	2.0	79.0	100.2	2.8	86
3.7	1.01	79.5	63.1	0.5	79.7	83.0	1.7	82.0	112.0	1.6	55
3.85	1.00	80.0	79.9	2.0	82.9	90.2	1.6	82.9	121.0	0.9	43

[a] The error limits for T_m and ΔH are about 1% and 5%, respectively.

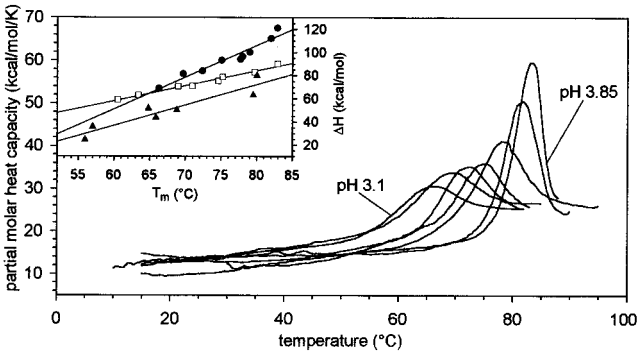

FIGURE 6: DSC scans of intact TmPGK at pH 3.1, 3.2, 3.3, 3.4, 3.5, 3.7, and 3.85 (from left to right). Insert: ΔH vs T_m plot for the first (▲), second (□), and third (●) transition of the DSC scans (ΔH_i and $T_{m,i}$ values result from the deconvolution of the DSC scans; cf. Table 3). The gradients of the linear regression yield $\Delta C_{p,1} = 1.8 \pm 0.6$ kcal mol^{-1} K^{-1} ($r^2 = 0.88$), $\Delta C_{p,2} = 1.3 \pm 0.2$ kcal mol^{-1} K^{-1} ($r^2 = 0.98$), and $\Delta C_{p,3} = 2.7 \pm 0.5$ kcal mol^{-1} K^{-1} ($r^2 = 0.94$), respectively.

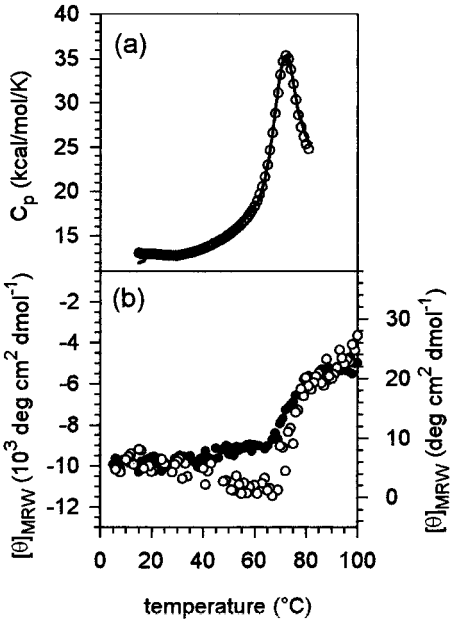

FIGURE 7: Temperature-induced transitions of TmPGK in 20 mM glycine/HCl, pH 3.3: (a) monitored by DSC (—) and fitted with a four-state model (○); (b) monitored by far- and near-UV CD [far-UV at 222 nm (●, left axis); near-UV at 285 nm (○, right axis)].

ascribed to the uncoupling of the domains (at ≈40 °C), followed by their sequential unfolding at 69 and 73 °C. DSC scans at pH 3.1 and 3.2 lack the first transition so that only the unfolding transitions of the domains are left. Plotting ΔH vs T_m for each transition, the data in Table 3 yield three

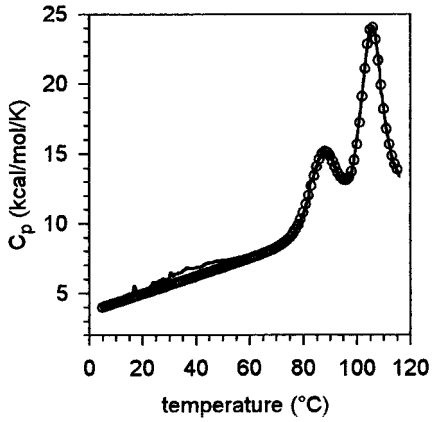

FIGURE 8: Temperature-induced transitions of N1/2 in 20 mM sodium phosphate, pH 7.0, monitored by DSC (—) and fitted with a three-state model (○).

straight lines (insert, Figure 6). The second and third transitions are well defined (including the data at pH 3.1 and 3.2); they result in $\Delta C_{p,2} = 1.3 \pm 0.2$ kcal mol^{-1} K^{-1} and $\Delta C_{p,3} = 2.7 \pm 0.5$ kcal mol^{-1} K^{-1}. $\Delta C_{p,1}$ can only be estimated because of the variations and the subjective choice of the pretransitional baseline; the result is $\Delta C_{p,1} = 1.8 \pm 0.6$ kcal mol^{-1} K^{-1}. If the pretransitional baseline is adjusted much steeper than observed in reality, the scans can be fitted by the three-state model over the whole pH range (*18*). The remaining transitions correspond to those of the second and third transition in the four-state fit.

Measurements at pH 7.0. In order to obtain thermodynamic information on the folding and stability under physiological conditions, DSC measurements were also performed at pH 7.0. Unfortunately, the thermal unfolding of PGK and C1/2 is irreversible, with transition temperatures at 101 and 97 °C, respectively. Thus, equilibrium thermodynamics cannot be applied. The thermal denaturation of N1/2 is about 70% reversible. It shows two clearly separated peaks with transition temperatures at 87.2 and 105. 2 °C (Figure 8) which can be fitted on the basis of a three-state model with $\Delta H_1 = 74.3$ kcal/mol, $\Delta H_2 = 116.7$ kcal/mol and $\Delta C_{p,1} = 0.9$ kcal mol^{-1} K^{-1}, $\Delta C_{p,2} = 1.8$ kcal mol^{-1} K^{-1}. Even without thermodynamic evaluation of the data, it is obvious that TmPGK as well as its isolated domains are stable beyond the optimal growth temperature of *Thermotoga maritima* around 80 °C.

GdmCl-induced equilibrium transitions of the isolated domains, monitored by fluorescence, are shown in Figure 9a,c. The unfolding of either domain is completely reversible at neutral pH and 20 °C. However, neither transition follows

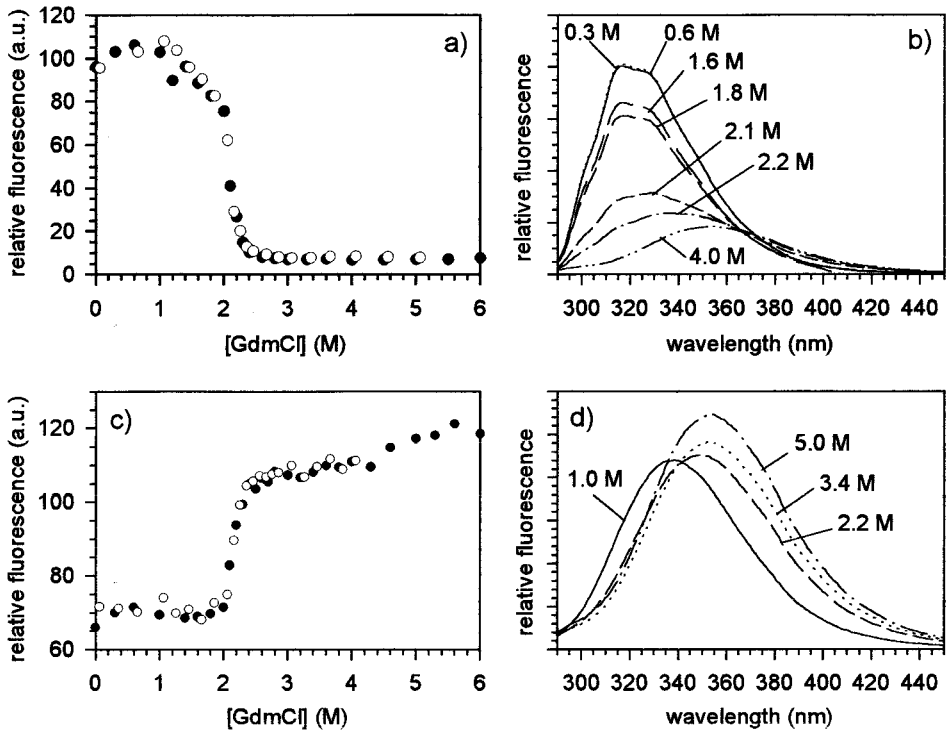

FIGURE 9: GdmCl-induced equilibrium denaturation (●) and renaturation (○) transitions of N1/2 (a) and C1/2 (c) monitored by fluorescence emission at 315 and 365 nm, respectively (λ_{exc} = 280 nm). Buffer: 20 mM sodium phosphate, pH 7.0, 20 °C. Selected fluorescence emission spectra of N1/2 (b) and C1/2 (d) at various GdmCl concentrations, measured with the same samples as used for the corresponding unfolding transition.

the two-state model, as indicated by the observation that at varying GdmCl concentrations the fluorescence emission does not yield an isospectric point (Figure 9b,d). This is in accordance with the DSC results at acidic pH. In contrast, the GdmCl-induced denaturation of the intact TmPGK at pH 7.0 is highly cooperative and follows a two-state transition (*13*). Similar differences in the mechanism of chaotropic denaturation have also been observed for other two-domain proteins, e.g., γB-crystallin (*19-21*).

DISCUSSION

In contrast to the thermal denaturation of yeast PGK, which has been shown to be irreversible in the absence of GdmCl (*10*−*12*, *22*, *23*), TmPGK and its N- and C-terminal domains undergo reversible unfolding transitions in the pH range between 3 and 4, allowing a thermodynamic treatment of the stability and folding of the hyperthermophilic enzyme and its constituent parts. The isolated domains unfold via partially structured intermediates, following a three-state model, N ⇔ I ⇔ U, in accordance with the results of the GdmCl-induced denaturation at pH 7. The structural analysis of the intermediates by near- and far-UV CD spectroscopy shows that $I_{N1/2}$ is altered in its tertiary structure but still maintains its native secondary structure. The structure of $I_{C1/2}$ cannot be characterized with certainty, as the two thermal transitions resulting from the deconvolution analyses are too close. Presumably, $I_{C1/2}$ consists of a folded and an unfolded subdomain, similar to the intermediate proposed for the isolated domains of the moderately thermophilic *Bacillus stearothermophilus* PGK (*24*−*26*). Here, equilibrium and kinetic intermediates of the N-terminal domain were shown to have extended secondary structure, whereas intermediates of the C-terminal domain were identified as folded subdomains that are subsequently paired in a rate-limiting step to form the native-like domain. During the folding of the isolated domains of yeast PGK, kinetic rather than equilibrium intermediates were observed (*27*).

The only model fitting the reversible thermal denaturation of intact TmPGK at pH 3.3−4.0 in a unique way suggests a three-step unfolding mechanism: N ⇔ I_1 ⇔ I_2 ⇔ U. Urea-induced denaturation at pH 3.7 (unpublished data) and the thermal denaturation assessed by CD spectroscopy confirm this model. The separate structural changes accompanying the three unfolding transitions at low pH can be characterized by making use of CD spectroscopy: N → I_1 is accompanied by a decrease in dichroic absorption at 285 nm, attributable to the loosening of domain contacts. The second and third transitions, I_1 → I_2 and I_2 → U, are not separable in the CD melting curves. Evidently, they affect both the tertiary and the secondary structures, suggesting sequential unfolding of the N- and C-terminal domains. In the DSC profiles at pH 3.1 and 3.2, the first transition is missing. The high-resolution structure of the intact enzyme (*8*, *9*) provides an explanation for these findings: At pH 3−4, aspartate and glutamate residues become titrated; in TmPGK, there are two ion pairs connecting the N- and C-termini (Glu2−Lys397, Lys3−Glu387) and three potential ion pairs in the domain interface (Arg62−Asp200, His150−Glu381, Glu174−His371), apart from ionic interactions in the interdomain helix (Glu172−Lys176, Glu174−Lys176). It may be assumed that the easily accessible Asp and Glu residues in the domain interface (and perhaps also at the N- and C-termini) are protonated first; thus, at pH <4, the domain contact in the intact enzyme becomes destabilized. Below pH 3.3, the protected Glu residues in the interdomain helix are titrated, causing

unfolding of the interdomain helix without affecting the structure of the domains. The latter state would correspond to the first intermediate in the denaturation at pH 3.3−4.0. Obviously, the apparent destabilization of the domains in intact TmPGK at low pH, compared to the stability of the isolated domains, is caused by alterations in the local charge distribution. At neutral pH, the opposite holds: Applying GdmCl as denaturant, the isolated domains of TmPGK are less stable than the intact molecule.

The proposed unfolding mechanism is a working hypothesis and requires further analysis. For yeast PGK, a similar scheme has been discussed (*21*, *28*). The question of which of the two domains exhibits higher stability is still unresolved. Comparing the enthalpy and heat capacity contributions of the domains in intact TmPGK with those observed for the isolated domains, the C-terminal domain seems to be more stable than the N-terminal one. For the yeast enzyme, in this context, contradicting results have been reported (*11*, *29*−*32*).

The above interpretation of the three unfolding transitions raises the question of why the isolated domains show two unfolding transitions whereas the domains in intact TmPGK show only one. One reason might be the choice of the domain border in the middle of helix h7 which leads to an increase in size for the isolated domains compared to the natural domains in TmPGK; as a consequence, additional local interactions may influence the modular structure and the stability of the domains (G. Auerbach, personal communication). As an alternative, the domains within the intact two-domain protein may unfold via intermediates with overlapping transitions not resolved by a sound deconvolution analysis.

Except for N1/2, due to the necessary reversibility, the free energy of stabilization was only determined at acidic pH. The results refer to single cooperative transitions. As the free energy depends on temperature, pH, and ionic strength, it is not feasible to compare the data for the three TmPGK transitions at acidic pH with those of PGKs from the other organisms, which were exclusively determined at neutral pH. For N1/2 in sodium phosphate, pH 7.0 and 25 °C, $\Delta G_1 = 7.6$ kcal/mol and $\Delta G_2 = 8.2$ kcal/mol were obtained. Comparing these values with those reported for the homologous N-terminal domain of the enzyme from the moderately thermophilic *B. stearothermophilus* under similar conditions ($\Delta G_1 = 5.2$ kcal/mol, $\Delta G_2 = 3.4$ kcal/mol) (*33*), the higher intrinsic stability of the hyperthermophilic TmPGK is obvious. Although no quantitative analysis of the free energy of TmPGK at neutral pH is feasible, the DSC scans for the irreversible heat denaturation clearly show that TmPGK is stable and maintains its native structure far beyond the physiological growth temperature of *T. maritima.*

ACKNOWLEDGMENT

Fruitful discussions with Drs. W. Pfeil, H. Schurig, and G. Auerbach are gratefully acknowledged. Katrin Zaiss thanks Drs. P. L. Mateo, V. V. Filimonov, and J. Ruiz-Sans (University of Granada, Spain) for their generous hospitality and kind introduction into the field of calorimetry.

REFERENCES

1. Jaenicke, R., Schurig, H., Beaucamp, N., and Ostendorp, R. (1996) *Adv. Protein Chem. 48*, 181−269.
2. Privalov, P. L. (1979) *Adv. Protein Chem. 33*, 167−241.
3. Privalov, P. L., and Potekhin, S. A. (1986) *Methods Enzymol. 131*, 4−51.
4. Freire, E., and Biltonen, R. L. (1978) *Biopolymers 17*, 463−479.
5. Makhatadze, G. I., and Privalov, P. L. (1995) *Adv. Protein Chem. 47*, 307−425.
6. Schurig, H., Beaucamp, N., Ostendorp, R., Jaenicke, R., Adler, E., and Knowles, J. (1995) *EMBO J. 14*, 442−451.
7. Beaucamp, N., Schurig, H., and Jaenicke, R. (1997) *Biol. Chem. 378*, 679−685.
8. Auerbach, G., Jacob, U., Grättinger, M., Schurig, H., and Jaenicke, R. (1997) *Biol. Chem. 378*, 327−329.
9. Auerbach, G., Huber, R., Grättinger, M., Zaiss, K., Schurig, H., Jaenicke, R., and Jacob, U. (1997) *Structure 5*, 1475−1483.
10. Hu, C. Q., and Sturtevant, J. M. (1987) *Biochemistry 26*, 178−182.
11. Brandts, J. F., Hu, C. Q., Lin, L. N., and Mas, M. T. (1989) *Biochemistry 28*, 8588−8596.
12. Galisteo, M. L., Mateo, P. L., and Sanchez-Ruiz, J. M. (1991) *Biochemistry 30*, 2061−2066.
13. Grättinger, M., Dankesreiter, A., Schurig, H., and Jaenicke, R. (1998) *J. Mol. Biol. 280*, 525−533.
14. Zaiss, K. (1998) Ph.D. Thesis, University of Regensburg.
15. Privalov, G. P., Kavina, V., Freire, E., and Privalov, P. L. (1995) *Anal. Biochem. 232*, 79−85.
16. Catazano, F., Graziano, G., Fusi, P., Tortora, P., and Barone, G. (1998) *Biochemistry 37*, 10493−10498.
17. McCrary, B. S., Edmondson, S. P., and Shriver, J. W. (1996) *J. Mol. Biol. 264*, 784−805.
18. Zaiss, K., Schurig, H., and Jaenicke, R. (1998) in *Biocalorimetry: Applications of Calorimetry in the Biological Sciences* (Ladbury, J., and Chowdhry, B. Z., Eds.) Chapter 21, pp 283−293, John Wiley & Sons, Ltd., Chichester, U.K.
19. Jaenicke, R. (1987) *Prog. Biophys. Mol. Biol. 49*, 117−237.
20. Rudolph, R., Siebendritt, R., Nesslauer, G., Sharma, A. K., and Jaenicke, R. (1990) *Proc. Natl. Acad. Sci. U.S.A. 87*, 4625−4629.
21. Jaenicke, R. (1999) *Prog. Biophys. Mol. Biol. 71*, 155−241.
22. Nojima, H., Ikai, A., Oshima, T., and Noda, H. (1977) *J. Mol. Biol. 116*, 429−442.
23. Nojima, H., and Noda, H. (1979) *J. Biochem. 86*, 1055−1065.
24. Hosszu, L. L. P., Craven, C. J., Parker, M. J., Lorch, M., Spencer, J., Clarke, A. R., and Waltho, J. P. (1997) *Nat. Struct. Biol. 4*, 801−804.
25. Parker, M. J., Sessions, R. B., Badcoe, I. G., and Clarke, A. R. (1996) *Folding Des. 1*, 145−156.
26. Parker, M. J., Spencer, J., Jackson, G.S., Burston, S. G., Hosszu, L. L. P., Craven, C. J., Waltho, J. P., and Clarke, A. R. (1996) *Biochemistry 35*, 15740−15752.
27. Missiakas, D., Betton, J. M., Chaffotte, A., Minard, P., and Yon, J. M. (1992) *Protein Sci. 1*, 1485−1493.
28. Lillo, M. P., Szpikowska, B. K., Mas, M. T., Sutin, J. D., and Beechem, J. M. (1997) *Biochemistry 31*, 250−256.
29. Freire, E., Murphy, K. P., Sanchez-Ruiz, J. M., Galisteo, M. L., and Privalov, P. L. (1992) *Biochemistry 31*, 250−256.
30. Gast, K., Damachun, G., Desmadril, M., Minard, P., Müller-Frohne, M., Pfeil, W., and Zirwer, D. (1995) *FEBS Lett. 358*, 247−250.
31. Sherman, M. A., Beechem, J. M., and Mas, M. T. (1995) *Biochemistry 34*, 13943−13948.
32. Beechem, J. M., Sherman, M. A., and Mas, M. T. (1995) *Biochemistry 34*, 13943−13948.
33. Parker, M. J., Spencer, J., and Clarke, A. R. (1995) *J. Mol. Biol. 253*, 771−786.

BI982447E